Counting Photons Emitted from Single Er Atoms in Energy Dispersive X-ray Spectroscopy

Kazu Suenaga[1], Toshiya Okazaki[1], Eiji Okunishi[2] and Syo Matsumura[3]

[1]Nanotube Research Center, National Institute of Advanced Industrial Science and Technology (AIST), Tsukuba 305-8565, Japan

[2]Electron Optics Division, JEOL Ltd. Akishima 196-8558, Japan

[3]HVEM Laboratory, Kyushu University, Fukuoka 819-0395, Japan

[4]Department of Applied Quantum Physics and Nuclear Engineering, Kyushu University, Fukuoka 819-0395, Japan

The characteristic x-ray signals from single Er atoms were successfully detected in energy dispersive x-ray spectroscopy (EDX). Highly focused electron probe in an aberration-corrected scanning transmission electron microscope (STEM) was used to excite the single Er atoms aligned in carbon cages, namely the peapod. The intensities of Er *L* and *M* lines from single Er atom were found to be ~ 10^5 times less than that of the *N*-edge of electron energy-loss spectroscopy (EELS), suggesting the intrinsic difficulty to sense single atoms in optical spectroscopy. Nevertheless, this work will certainly ensure the possibilities to obtain optical spectra from single atoms and to estimate the fluorescent yield at single atom basis, therefore the technique will likely find wide fields of applications in nano-physics research.

Highly sensitive spectroscopy will become a key procedure to diagnose nano-scale devices, while the single atom detection has been believed very difficult to realize in optical spectroscopy. Electron microscopes are widely used to investigate the nano-objects with high spatial resolution. Recently, an extremely tiny probe (~ 0.1 nm) with high current becomes available in aberration corrected scanning transmission electron microscope (STEM). Using such a highly focused probe the individual atoms can be excited in nano-scale devices. Therefore, the analysis of the element-specific signals gives direct information for the chemical species and electronic structures of examined specimens with atomic precision.

In earlier studies, the electron energy-loss spectroscopy (EELS) was used to detect the single atoms of lanthanide metals (1, 2, 3, 4) as well as light elements such as carbon (5). Chemical analysis by means of EELS has, however, a limitation of its applicability because the elements detectable are limited. The noble metals such as gold or platinum for example are difficult to be detected in EELS with high sensitivity. This is a severe drawback of EELS for some research fields which treat a very small number of noble metal atoms such as the meteorite, catalytic clusters or anti-cancer drug. On the other hand, the chemical analysis by means of the characteristic x-ray signals (energy dispersive x-ray spectroscopy, EDX) allows us chemical information for wider range of elements, typically from B to U. However, the single atom detection by means of EDX has been considered to be more difficult because the photoemission is strongly reduced by the fluorescent yield as well as the inelastic cross-section. More apparently, the detection efficiency for x-ray in TEM is generally quite low because of the limitation in the solid angle (typically 0.3 sr) for typical EDX detector, while most of the scattered electron can be counted in case of the EELS in transmission. We demonstrate here the first EDX experiment to sense the single atoms.

There is another important advantage in EDX over EELS in terms of the signal delocalization. Even though a small electron probe (0.1 nm) can be routinely delivered by an aberration-corrected STEM, spatial resolution of the chemical analysis is indeed limited by the delocalization effect of EELS and EDX signals, which could smear out the chemical maps of atomic resolution (6, 7, 8). The EDX and EELS signals are both originated to the inelastic scattering events, and intrinsically affected by the signal delocalization. The degree of delocalization is determined by the impact parameter (b) which is expressed as $b = hv/\Delta E$, where v is the incident electron velocity and ΔE is the core-depth for the inelastic event (or the energy-loss in EELS). Therefore there are only two ways to reduce the delocalization effect; to slow the incident electron (lower the accelerating voltage) or to use the deeper core-loss edge (8). The typical core-loss used by EELS is up to 1 keV (or ~ 2 keV at most), while the EDX can utilize the spectra upto 10 ~ 20 keV (or 30

keV). One can reduce the delocalization effect by a factor of ten if a proper core-shell is chosen for EDX chemical mapping in comparison to the EELS edge.

The specimen must be carefully chosen for the single atom detection in EDX experiment. The excited volume which all the incident electrons can be absorbed indeed determines the spatial resolution of the EDX analysis in a bulk case (9). The ideal specimen is a series of single atoms which are well-aligned in line with a regular interval and the specimen support should be as thin as possible. Eventually we have chosen the metallofullerene peapods as the test specimen (1). Er@C_{82} peapods were used here. They contain heavy atoms (Er) inside the carbon cages (C_{82}) which allow each metal atom align with a moderate interval (~ 1.1 nm) in a single-walled carbon nanotube. The specimen is extremely thin (~ 1.5 nm thick in diameter) and provides an ideal support (see Fig. 1b). Er is also detectable by EELS therefore we can directly compare the detection efficiency of EDX and EELS. The simultaneous EELS can allow us to account the number of inelastic events, therefore the fluorescent yield of single Er atoms can be directly estimated by a ratio of EDX and EELS intensities.

To avoid the severe electron beam damage during the experiment, the microscope must be operated at the lower accelerating voltage. On the other hand, the probe should be small enough to discriminate the adjacent single atoms in the specimen. Furthermore, the probe current should be as high as possible because the counting efficiency of the emitted photons is expected very low. We used a scanning transmission electron microscope (JEM ARM200F) equipped with a CEOS hexapole type Cs corrector (CESCORR). A silicon drift detector (SSD) with 100 mm^2 detection area (Centurio, JEOL Ltd.) was used for counting the X-ray signals. This device allows a large solid angle (~ 0.8 sr.) for the EDX signal acquisition within the ultra-high resolution polepiece (2.0 mm gap). The accelerating voltage was set to 60kV in a compromise among the possible irradiation damage induced by the electron beam and the attainable probe current and size. A post-column electron spectrometer (Gatan Imaging Filter, GIF Quantum) was used for the simultaneous EELS acquisition. The experimental setup is summarized in Fig. 1a. When the convergence angle of the incident electron beam (α) is ~ 40 mrad, the beam current reaches ~ 200 pA in a 0.15 nm probe. The entrance angle of the EELS spectrometer (β) is ~ 50 mrad. The SWNTs specimens encapsulating metallofullerenes were dispersed in hexane and dropped onto a lacey carbon mesh on Mo grid.

Fig. 2(a) shows an ADF image of the examined metallofullerene peapods. Each brighter spot corresponds to single Er atom and is aligned with a regular interval. The yellow dotted line shows where the incident electron probe scans across an Er atom (from up to down). 80 pairs of EDX and EELS spectra were simultaneously acquired with the constant increment along the line.

The acquisition time for each probe position is 0.5 sec. Fig. 2(b)(c) show EDX and EELS spectra extracted from the line-scan. 10 spectra are summed up for each. The EDX spectrum clearly shows the peaks of Er *M*-line and Er *L*(α)-line (indicated by the solid arrows) at 1.4keV and 6.9 keV, respectively. The open arrows show two extra peaks which correspond to Mo/S and Cl. Mo signal is from the microscopy grid used for this experiment and S is probably due to the carbon disulfide (CS_2) solvents which were used when the metallofullerene molecules were dispersed. Cl is a trace of HCl acid that was used to purify the original SWNTs. The y axis is the number of counted photons and the maximum peak height is around 10 counts for Er M and L-lines. Note that the counts do not increase monotoneously even when the acquisition time is extended. This means that the Er atom is not completely immobile during the acquisition and that it can be often kicked out by the intense electron beam (3, 4). Simultaneously recorded EELS spectrum unambiguously shows the Er *N*-edge. The SN ratio is quite high to isolate the edge for EELS recorded even at the same acquisition time for EDX.

Fig. 3 shows line-profiles of the intensities of EDX, EELS and ADF recorded across the Er atom. Note that there was a small specimen drift during the experiment and therefore the scanning distance is slightly shortened. The x axis is the probe position after the drift compensation. The Er *L* and *M* profiles are largely scattered and the maximum numbers of counted photons are very small (10 to 20 counts). In spite of this counting inefficiency, both profiles clearly show a maximum during the line-scan, which corresponds to the Er atomic position. They coincide with the maxima of the EELS *N*-edge and the ADF intensities. If we compare the counting statistics, the EELS *N*-edge shows more than 5×10^5 electron counts for the *N*-edge after the standard background subtraction, while the EDX has only 10 or 20 photon counts. The single atom detection by means of EDX is extremely disadvantageous in comparison with the EELS by 5 orders of magnitude in terms of the signal counts. Note that the image-spectrum to make a two dimensional map for EDX was not feasible because of the strong irradiation damage due to the very high probe current.

Because the EDX and EELS spectra were simultaneously recorded in the same acquisition time and with the same probe current, the same number of the inelastic scattering events should have been involved. In this condition, one can directly compare the counting efficiency in the single atom detection in EDX and EELS chemical analysis. Since the specimen is quite thin, most of the inelastically scattered electrons were forward-scattered and then entered into the EELS spectrometer (6). Characteristic x-ray signal (the number of detected photons) estimated as the intensity of the specific EDX line can be compared with the characteristic EELS signal as following (6);

$$I_{EDX(M)}/I_{EELS(N)} = \eta\omega_M \ (\sigma_M/\sigma_N) \exp(t/\lambda_e)$$

where $I_{EDX(M)}$ and $I_{EELS(N)}$ are the signals for EDX *M*-line and EELS *N*-edge, η is the EDX collecting efficiency for the EDX detector, ω_k is the fluorescent yield for k shell, and σ_k is the inelastic cross-section for k-shell. The ratio of specimen thickness to the elastic mean free path (t/λ_e) can be regarded as zero because the specimen is quite thin in our experiment. The inelastic cross-section ratio (σ_M/σ_N) between *N* and *M* edges is estimated as ~ 0.01 with the Hartree-Slater model, and the collecting efficiency η is roughly equal to the solid angle ratio (0.80 sr /4π ~ 0.064). These values calculate the ω_M as ~ 0.03 which is quite reasonable for the photon energy at 1,400 eV.

The atomic resolution EDX maps of crystals have been recently reported by a few groups (10, 11, 12) . These successful chemical mappings are associated with the strong channeling effect in which the most of the incident electrons can travel through the atomic columns. Also at least several tens of atoms are contributing to their EDX signals. Therefore the atomic resolution is more easily feasible in their bulk crystals and the delocalization effect is not very much pronounced. In case of our experiment in which the thinnest specimen was used and no channeling effect was involved, the spatial resolution can be directly represented by a mixture of the probe size and delocalization effect (6).

The delocalization of inelastic scattering should be smaller for the deeper core-loss signals as described above. We therefore expect sharper atomic profile in the Er *L* than Er *N*-edge. The difference can be hardly seen between the Er *L* and *M* lines. Larger tail in the Er *N*-edge EELS can be recognized due to the delocalization effect and the probe tail. Quantitative comparison of the EELS profile with the tails of EDX profiles is not feasible because of the extremely low counting statistics of EDX signals. Note that the ADF intensity does not directly reflect the Er atomic profile because it involves the contribution of carbon cage and nanotubes as well.

The importance of this experiment also lies in the successful detection of residual S and Cl in EDX spectra. They are the trace of solvents (CS_2) or acid (HCl) used for specimen preparation. It was not easy to detect them by EELS even though the sulfur *L*-edge (~ 165eV) and chlorine *L*-edge (~ 200eV) are in the range of the viewed energy window. The intense Er *N*-edge (~ 168 eV) overlaps the both edges and hampers their visibilities. This experiment is therefore an excellent demonstration of EDX capability to detect very small amount of unforeseen elements, such as impurities or contaminants, with well separated core-shell lines.

The present EDX experiment cannot be regarded as the simple alternative of EELS. To sense single atoms in optical spectroscopy would provide distinct information from those delivered

by EELS fine structure analysis. Especially measuring the optical response of individual quantum object (13), or even individual atoms, is now indeed foreseen. Also the soft x-ray emission spectroscopy or wavelength dispersive x-ray spectroscopy would provide useful information about the occupied valence states (14) when it is performed with atomic sensitivity. Practically the technique shown in this work will find quick applications to the other important research fields because of its applicability to the noble metal. For instance, detecting the small amount of Pt and Ir would be greatly desired in geophysical research associated with meteorites. And measuring the actual composition of Au or Pt based alloy catalysts provides most important insights in catalytic industries for fuel cells. Combined with molecular imaging technique it may be anticipated to investigate how Pt complex molecule interacts with the nucleotides sequence of DNA, which would give direct information for the function of the anti-cancer drug at molecular level.

This work was partly performed on the Nanotechnology Network Japan program sponsored by MEXT of the Japanese Government. Ms. Yoko Iizumi and Yoshiko Niimi are gratefully acknowledged for their help in specimen preparations. KS also acknowledges a support from the Grant-in-Aid for Scientific Research from MEXT (19054017).

(1) K. Suenaga et al., Science 290 (2000) 2280-2282
(2) M. Varela et al., Phys. Rev. Lett. 92 (2004) 095502
(3) K. Suenaga et al., Nature Chem. 1 (2009) 415-418
(4) O. Krivanek et al., Ultramicrosc., 110 (2010) 935-945
(5) K. Suenaga and M. Koshino, Nature 468 (2010) 1088-1090
(6) R. Egerton, in *Electron Energy-Loss Spectroscopy in the Electron Microscope* 3rd Ed. Springer, New York, (2011)
(7) D. Muller and J. Silcox, Ultramicrosc. 59 (1995) 195
(8) K. Suenaga, Y. Iizumi and T. Okazaki, Euro. Phys. J.: Appl. Phys. 54 (2011) 33508
(9) M. Watanabe, Chapter 7 in *Scanning Transmission Electron Microscopy, Imaging and Analysis*, Ed. S. J. Pennycook and P. D. Nellist, Springer New York, (2011) pp. 291-351
(10) M.-W. Chu, S. C. Liou, C.P. Chang, F.-S. Choa and C.H. Chen, Phys. Rev. Lett., 104 (2010) 196101
(11) M. Watanabe, M. Kanno and E. Okunishi, JEOL News 45, 8 (2010)
(12) A.J. d'Alfonso, B. Freitag, D. Klenov and L.J. Allen, *Phys. Rev. B* **81**, (2010)100101
(13) L. Zagonel et al., Nano Lett. 11 (2011) 568-573
(14) M. Terauchi et al., J. Electron Microsc., 10.1093/jmicro/dfr076 (online)

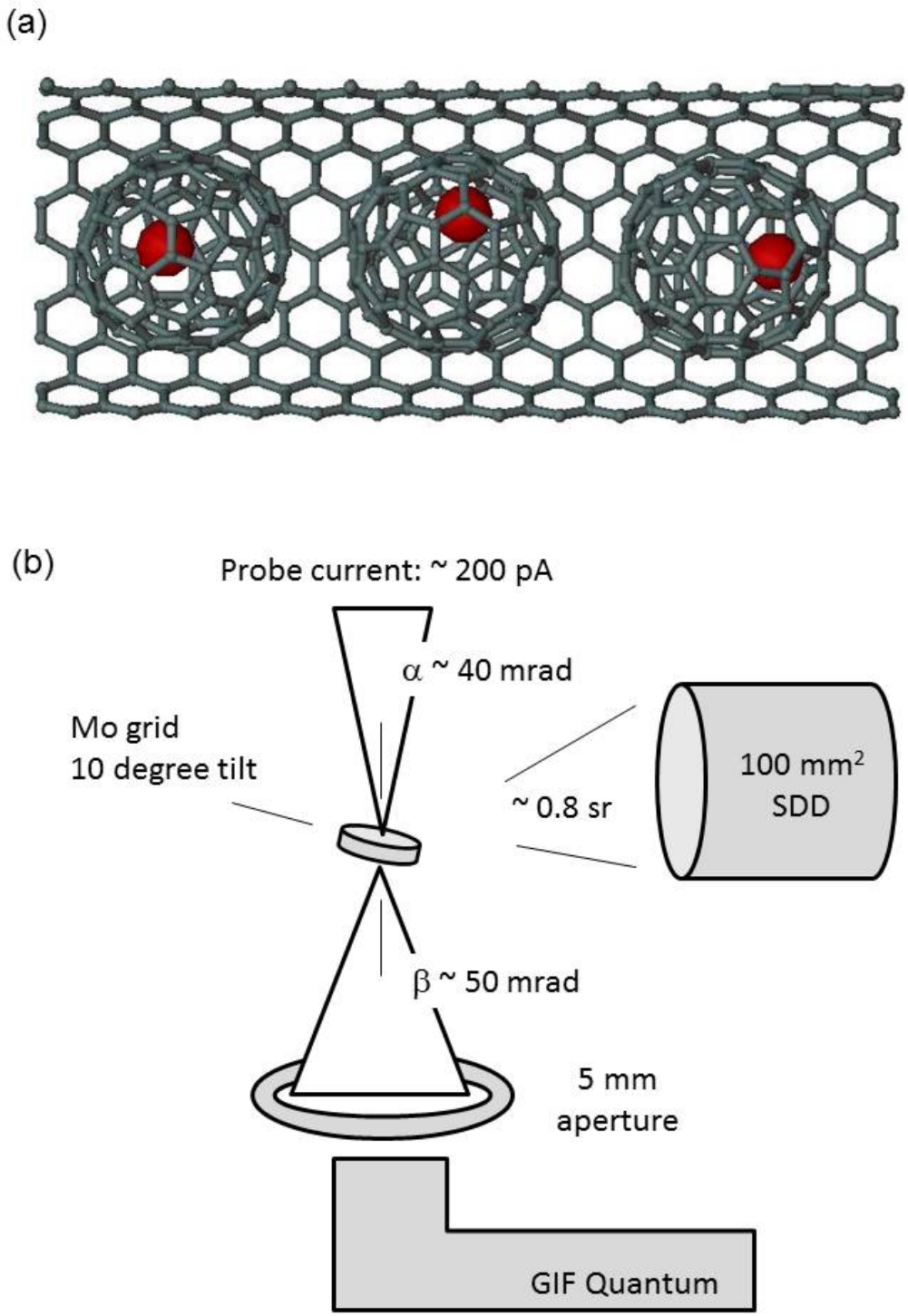

Fig. 1 (a) The schematic presentation of the peapod specimens. Each fullerene cage (C_{82}) carries single Er atom and is aligned inside SWNT. Red: Er and Gray: carbon. (b) Experimental set up used for the simultaneous EDX and EELS chemical analyses. The SDD is located at the side of specimen

with the solid angle (0.80 sr), while the EELS signal is recorded in transmission.

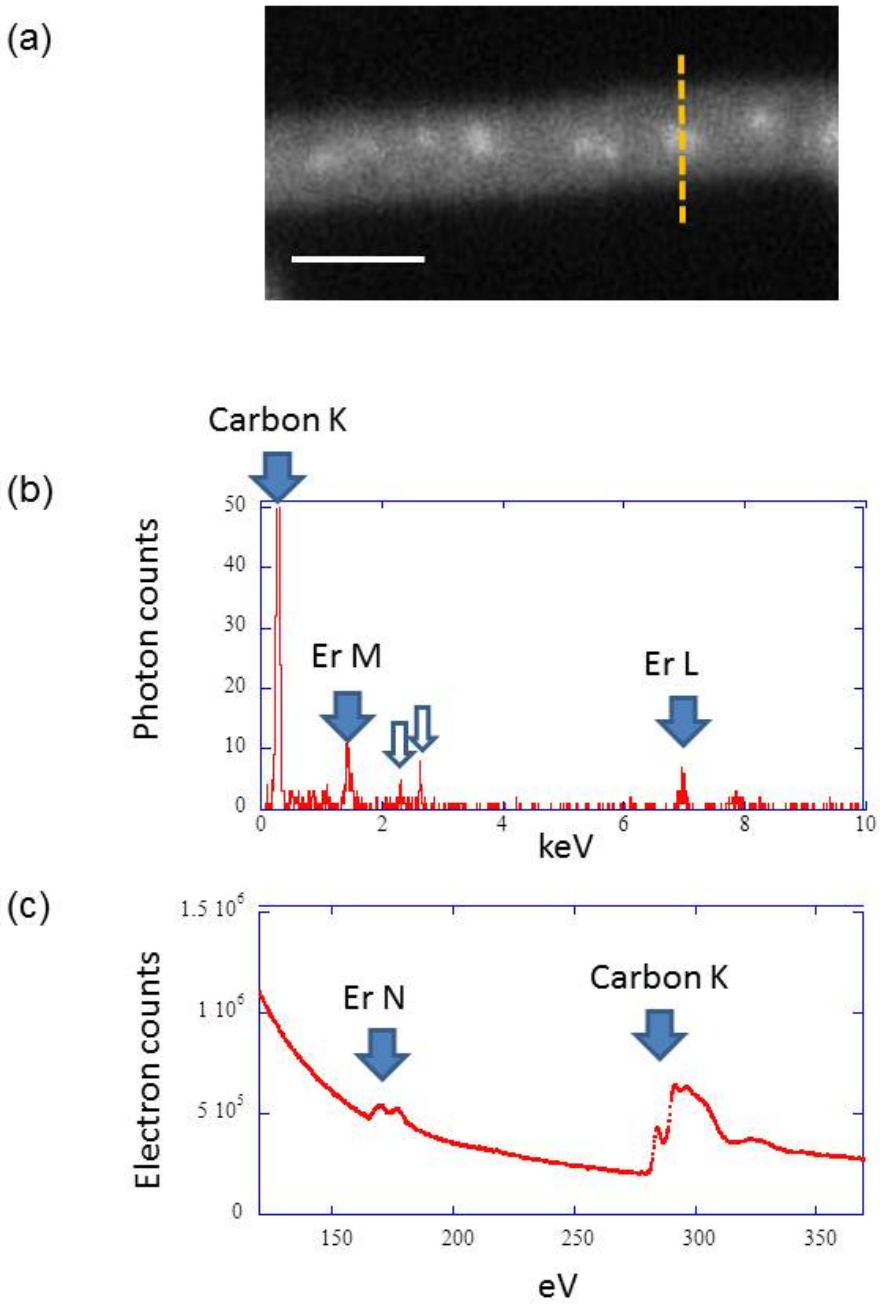

Fig. 2 (a) An ADF image of the specimen. The brighter spots correspond to single Er atoms and well distributed with 1 nm interval in average. The yellow dotted line shows where a typical line-spectra

was recorded. Scale bar = 2nm. (b) An EDX spectrum recorded from the line-scan. 10 spectra were summed up. Er M and Er L lines were clearly visible as well as carbon K line (solid arrows). Open arrows shows Mo, S and Cl signals due to the Mo grid or the solvent used for the specimen preparation (carbon disulfide and hydrochloric acid). (c) An EELS spectrum recorded simultaneously with the EDX spectrum above. The Er N edge shows very high SN ratio.

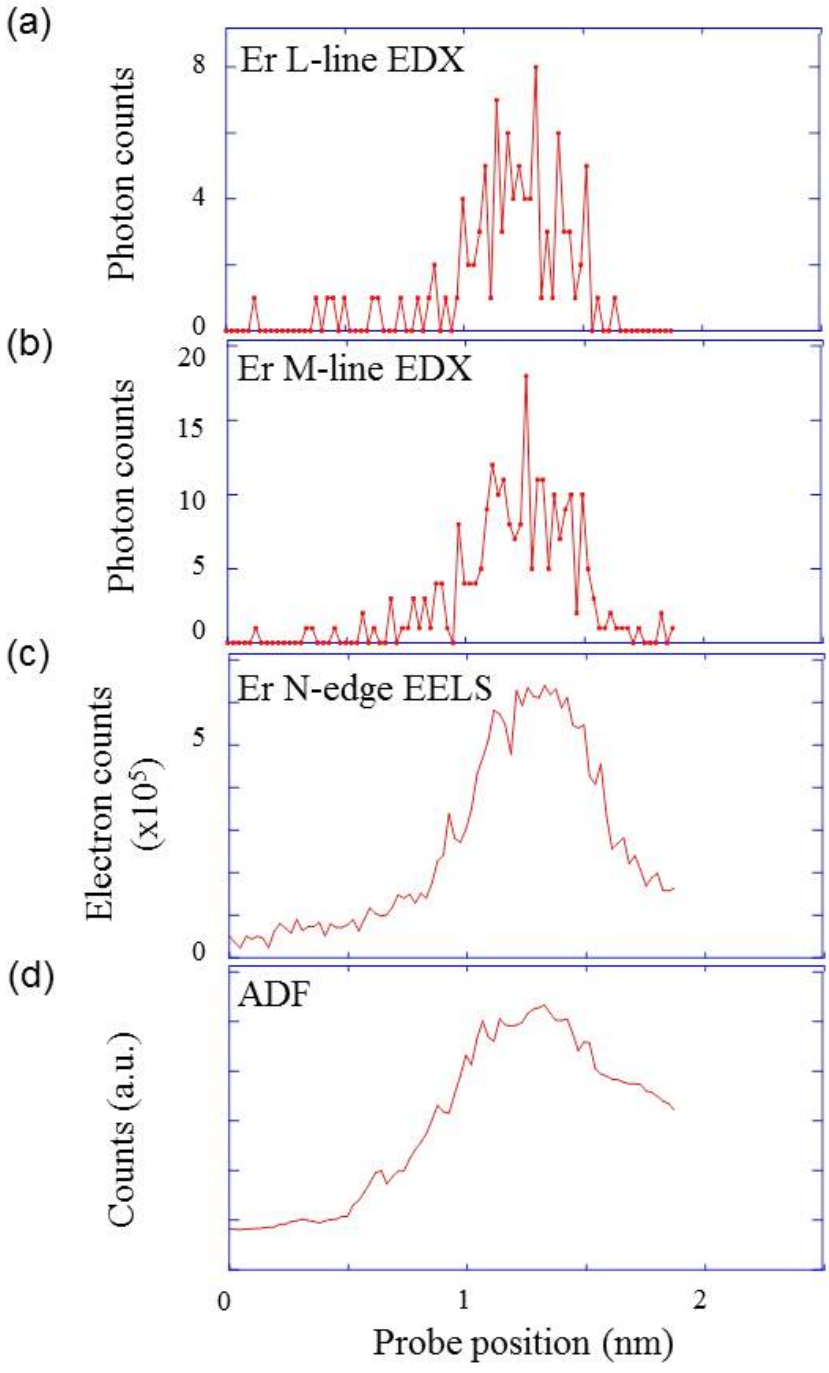

Fig. 3 (a-d) Line profiles from the line-scan across a single Er atom for Er L (EDX), Er M (EDX), Er N (EELS) and ADF, respectively. The photon counts for Er L and M EDX signals are around 8 and 18 counts at maximum. Note that the transmission EELS can provide 10^5 times better signals as the number of electron suffered the inelastic scattering. One can notice a larger tail for Er N EELS

signals than those for EDX ones, which may reflect the different delocalization effects. Note that the line-scan was not completely performed along the yellow dotted line due to a possible specimen drift during the acquisition. The x axis of the figures is then compensated.